

Principle of Maximum Entropy Applied to Rayleigh-Bénard Convection

Takafumi Kita

Department of Physics, Hokkaido University, Sapporo 060-0810, Japan

(dated: March 23, 2024)

A statistical-mechanical investigation is performed on Rayleigh-Bénard convection of a dilute classical gas starting from the Boltzmann equation. We first present a microscopic derivation of basic hydrodynamic equations and an expression of entropy appropriate for the convection. This includes an alternative justification for the Oberbeck-Boussinesq approximation. We then calculate entropy change through the convective transition choosing mechanical quantities as independent variables. Above the critical Rayleigh number, the system is found to evolve from the heat-conducting uniform state towards the convective roll state with monotonic increase of entropy on the average. Thus, the principle of maximum entropy proposed for nonequilibrium steady states in a preceding paper [T. Kita: J. Phys. Soc. Jpn. 75 (2006) 114005] is indeed obeyed in this prototype example. The principle also provides a natural explanation for the enhancement of the Nusselt number in convection.

I. INTRODUCTION

In a preceding paper,¹ we have proposed a principle of maximum entropy for nonequilibrium steady states: The state which is realized most probably among possible steady states without time evolution is the one that makes entropy maximum as a function of mechanical variables. We here apply it to Rayleigh-Bénard convection of a dilute classical gas to confirm its validity.

Rayleigh-Bénard convection is a prototype of nonequilibrium steady states with pattern formation, and extensive studies have been carried out to clarify it.^{2,3,4,5,6,7,8,9} However, no calculation seems to have been performed on entropy change through the nonequilibrium "phase transition," despite the fact that entropy is the key concept in equilibrium thermodynamics and statistical mechanics. There may be at least four reasons for it. First, there seems to have been no established expression of nonequilibrium entropy. Second, the standard starting point to describe Rayleigh-Bénard convection is a set of deterministic equations for the particle, momentum and energy flows, with all the thermodynamic effects pushed into phenomenological parameters of the equations.^{2,6} Third, one additionally adopts the Oberbeck-Boussinesq approximation to the equations in the conventional treatment.^{2,6,10} Despite many theoretical efforts over a long period,^{11,12,13,14,15} a well-accepted systematic justification for it seems still absent, thereby preventing a quantitative estimation of entropy change. Fourth, there is ambiguity on what to choose as independent variables of entropy for open systems.

In a preceding paper,¹ we have derived an expression of nonequilibrium entropy together with the evolution equations for interacting bosons/fermions. We here apply them to a classical gas of the dilute high-temperature limit where the evolution equations reduce to the Boltzmann equation. We carry out a microscopic derivation of the hydrodynamic equations for the particle, momentum and energy densities (i.e., the basic conservation laws) from the Boltzmann equation. We then provide a systematic justification for the Oberbeck-Boussinesq approximation to describe the convection. With these preliminaries,

we perform a statistical-mechanical calculation of entropy change through the convective transition by choosing mechanical quantities as independent variables. It is worth pointing out that classical gases have been used extensively for detailed experiments on Rayleigh-Bénard convection over the last two decades.^{5,8,9} Thus, quantitative comparisons between theory and experiment are possible here.

This paper is organized as follows. Section II derives (i) equations of motion for the particle, momentum and energy densities and (ii) an explicit expression for the distribution function f , both starting from the Boltzmann equation. Section III reduces the equations of xII in a way appropriate to treat Rayleigh-Bénard convection of a dilute classical gas. This includes a systematic justification of the Oberbeck-Boussinesq approximation and a derivation of the expression of entropy for convection. Section IV transforms the equations of xIII into those suitable for periodic structures with the stress-free boundaries. Section V presents numerical results obtained by solving the equations of xIV. It is shown explicitly that the principle of maximum entropy is indeed obeyed by the convection. Concluding remarks are given in xVI.

II. DISTRIBUTION FUNCTION, CONSERVATION LAWS AND ENTROPY

A. The Boltzmann equation and entropy

We shall consider a monatomic dilute classical gas under gravity. This system may be described by the Boltzmann equation:^{16,17}

$$\frac{\partial f}{\partial t} + \frac{\mathbf{p}}{m} \cdot \frac{\partial f}{\partial \mathbf{r}} - m \mathbf{g} \cdot \frac{\partial f}{\partial \mathbf{p}_z} = C : \quad (1)$$

Here $f = f(\mathbf{p}; \mathbf{r}; t)$ is the distribution function, t the time, \mathbf{p} the momentum, m the mass, \mathbf{r} the space coordinate, and \mathbf{g} the acceleration of gravity. With a unified description of classical and quantum statistical mechanics in mind, we choose the normalization of f such that it is

dimensionless and varies between 0 and 1 for fermions. The collision integral C is given explicitly by

$$C(p; r; t) = \frac{1}{(2\pi)^3} \int d^3p_1 \frac{1}{(2\pi)^3} \int d^3p_0 \frac{1}{(2\pi)^3} \int d^3p_1^0 V_{p^0 p} \int d^3p_1^0 (f_{p^0} f_{p_1^0} - f_p f_{p_1}) \quad (2)$$

where V_q is Fourier transform of the interaction potential and $E_p = p^2/2m$.

Equation (1) also results from eq. (63) of ref. 1 as follows: (i) approximate the spectral function as $A(p; r; t) = 2\pi \delta(E_p - m g z)$; (ii) substitute the second-order self-energy of eq. (66) into the collision integral of eq. (64); (iii) take the high-temperature limit; and (iv) integrate eq. (63) over p to obtain an equation for

$$f(p; r; t) = \frac{1}{2\pi} \int d^3p A(p; r; t) f(p; r; t) \quad (3)$$

This whole procedure amounts to treating the interaction potential only as the source of dissipation in the dilute high-temperature limit, thus neglecting completely its influence on the density of states, i.e., on the real part of the self-energy.

With a change of variables $p_1 = p + q$, $p_0 = P - q^0/2$ and $p_1^0 = P + q^0/2$ in eq. (2), the collision integral is transformed into

$$C = \frac{1}{(2\pi)^3} \int d^3q \frac{1}{m} \int d^3q^0 [f_{p+q} f_{p-q^0/2} - f_p f_{p+q}] \quad (4)$$

where $d = d^3q^0 d^3q / (q^0 - q) m \int d^3q^0 \int d^3q$ is the differential cross section in the center-of-mass coordinate of the scattering with d^3q^0 denoting the infinitesimal solid angle. We shall use the contact interaction with no q dependence in V_q , where d reduces to

$$d = a^2 d^3q^0 d^3q / (q^0 - q); \quad (5)$$

with $a = m \int d^3q^0 \int d^3q$ denoting the scattering length. Now, the differential cross section acquires the form of the two-particle collision between hard-sphere particles with radius a .¹⁸

Entropy per unit volume is given in terms of f by

$$S = \frac{k_B}{V} \int d^3p \frac{1}{(2\pi)^3} f (\log f - 1); \quad (6)$$

with V denoting the volume. This expression also results from eq. (69) of ref. 1 for entropy density by: (i) adopting the quasiparticle approximation $A(p; r; t) = 2\pi \delta(E_p - m g z)$; (ii) defining f by eq. (3) above; (iii) taking the high-temperature limit; and (iv) performing integration over r . The term -1 in the integrand of eq. (6) is absent in the Boltzmann H-function¹⁶ but naturally results from the procedure (iii) above. Indeed, eq. (6) reproduces the correct expression of entropy in equilibrium.¹⁹

B. Conservation laws

We next consider conservation laws which originate from the Boltzmann equation. The basic physical quantities relevant to them are the density $n(r; t)$, the velocity $v(r; t)$, the temperature $T(r; t)$, the momentum flux density tensor $\underline{\underline{P}}(r; t)$ in the reference frame moving with the local velocity v , and the heat flux density $j_Q(r; t)$. They are defined by

$$n(r; t) = \frac{1}{(2\pi)^3} \int d^3p f(p; r; t); \quad (7a)$$

$$v(r; t) = \frac{1}{n(r; t)} \frac{1}{(2\pi)^3} \int d^3p \frac{p}{m} f(p; r; t); \quad (7b)$$

$$T(r; t) = \frac{2}{3k_B n(r; t)} \frac{1}{(2\pi)^3} \int d^3p \frac{p^2}{2m} f(p; r; t); \quad (7c)$$

$$\underline{\underline{P}}(r; t) = \frac{1}{(2\pi)^3} \int d^3p \frac{p p}{m} f(p; r; t); \quad (7d)$$

$$j_Q(r; t) = \frac{1}{(2\pi)^3} \int d^3p \frac{p^2}{2m} \frac{p}{m} f(p; r; t); \quad (7e)$$

with $p = p - m v$. The expressions 7a)–7e) also result from eqs. (C 1a), (C 1b), (C 20a), (C 14) and (C 20b) of ref. 1, respectively, by noting eq. (3), neglecting the interaction terms, and identifying the local internal-energy density E' as $E' = \frac{3}{2} n k_B T$.

To obtain the number, momentum and energy conservation laws, let us multiply eq. (1) by 1, p and $p^2/2m$, respectively, and perform integration over p . The contribution from the collision integral (2) vanishes in all the three cases due to the particle, momentum and energy conservations through the collision.^{16,17} The resulting hydrodynamic equations can be written in terms of the quantities of eq. (7) as

$$\frac{\partial n}{\partial t} + r \cdot (n v) = 0; \quad (8a)$$

$$\frac{\partial v}{\partial t} + v \cdot r v + \frac{1}{m n} r \cdot \underline{\underline{P}} + g e_z = 0; \quad (8b)$$

$$\frac{3}{2} n k_B \frac{\partial T}{\partial t} + v \cdot r T + r \cdot j_Q + \underline{\underline{A}} : \underline{\underline{B}} : r v = 0; \quad (8c)$$

where e_z is the unit vector along the z axis and $\underline{\underline{A}} : \underline{\underline{B}}$ denotes the tensor product: $\underline{\underline{A}} : \underline{\underline{B}} = A_{ij} B_{ji}$. These equations are identical in form with eqs. (C 2), (C 9) and (C 21) of ref. 1, respectively, with $U = m g z$ and $E' = \frac{3}{2} n k_B T$.

C. The Enskog series

We now reduce the whole procedures of solving eq. (1) for $(p; r; t)$ to those of solving eq. (8) for $(r; t)$. We adopt the well-known Enskog method^{16,17} for this purpose, i.e., the expansion from the local equilibrium. We here describe the transformation to the extent necessary for a later application to Rayleigh-Benard convection.

Let us expand the distribution function formally as

$$f(p; r; t) = f^{(eq)}(p; r; t) + \epsilon f^{(1)}(p; r; t) + \dots; \quad (9)$$

where $f^{(eq)}$ is the local-equilibrium distribution given explicitly by

$$f^{(eq)} = \frac{(2\pi)^{-3} n}{(2\pi m k_B T)^{3/2}} \exp \left(-\frac{p^2}{2m k_B T} \right); \quad (10)$$

with $p = m v$. This $f^{(eq)}$ has been chosen so as to satisfy the two conditions:^{16,17} (i) the local equilibrium condition that the collision integral vanishes; (ii) eqs. (7a)–(7c) by itself. It hence follows that the higher-order corrections $f^{(j)}$ ($j = 1, 2; \dots$) in eq. (9) should obey the constraints:

$$\int \frac{d^3 p}{(2\pi)^3} p^n f^{(eq), (j)} = 0 \quad (n = 0, 1, 2); \quad (11)$$

Note that we have incorporated the space-time dependent parameters in $f^{(eq)}$, i.e., n , v and T , which can be determined completely with eqs. (8a)–(8c) of conservation laws. The remaining task here is to express the extra quantities \hat{r} and \hat{j}_Q in eq. (8) as functionals of n , v and T .

Let us substitute eq. (9) into eq. (1), regard the space-time differential operators on the left-hand side as first-order quantities, and make use of the fact that the collision integral (2) vanishes for $f^{(eq)}$. We thereby arrive at the first-order equation:

$$\frac{\partial f^{(eq)}}{\partial t} + \frac{p}{m} \frac{\partial f^{(eq)}}{\partial r} + \frac{p_z g}{k_B T} f^{(eq)} = C^{(1)}; \quad (12)$$

where $C^{(1)}$ is obtained from eq. (4) as

$$C^{(1)} = \int \frac{d^3 q}{(2\pi)^3} \frac{q}{m} \int d f_p^{(eq)} f_{p+q}^{(eq)} \left[\begin{aligned} & \hat{r}_{p+(q-q^0)=2}^{(1)} + \hat{r}_{p+(q+q^0)=2}^{(1)} - \hat{r}_p^{(1)} - \hat{r}_{p+q}^{(1)} \end{aligned} \right]; \quad (13)$$

With eq. (10), the derivatives of $f^{(eq)}$ in eq. (12) are transformed into those of n , v and T . We then remove the time derivatives by using eq. (8) in the local-equilibrium approximation, where

$$\frac{\partial f^{(eq)}}{\partial t} = P \mathbf{1}; \quad \hat{j}_Q^{(eq)} = 0; \quad (14)$$

with $P = nk_B T$ the pressure and $\mathbf{1}$ the unit tensor. The left-hand side of eq. (12) is thereby transformed into

$$\begin{aligned} & \frac{\partial f^{(eq)}}{\partial t} + \frac{p}{m} \frac{\partial f^{(eq)}}{\partial r} + \frac{p_z g}{k_B T} f^{(eq)} \\ &= f^{(eq)} \left[2 k k \frac{k^2}{3} \mathbf{1} : \hat{r} v + k^2 \frac{5}{2} \frac{p}{m} \hat{r} \ln T \right]; \end{aligned} \quad (15)$$

with k a dimensionless quantity defined by

$$k = \frac{p}{\sqrt{2m k_B T}}; \quad (16a)$$

It is convenient to introduce the additional dimensionless quantities:

$$\hat{v} = \frac{r}{\sqrt{\frac{m}{2k_B T}}} v; \quad \hat{r} = n^{1/3} r; \quad (16b)$$

and the mean-free path:

$$\lambda = \frac{1}{4\pi^2 a^2 n}; \quad (17)$$

Using eqs. (16) and (17) and noting eqs. (5), (10), (13) and (15), we can transform eq. (12) into the dimensionless form:

$$\begin{aligned} & \frac{2}{\pi} \frac{p}{\lambda} \frac{1}{2} \int \frac{d^3 q}{4} \frac{d^3 q^0}{4} \frac{(q^0 - q)}{q} e^{k^2 (k+q)^2} \\ & \left[\hat{r}_{k+(q-q^0)=2}^{(1)} + \hat{r}_{k+(q+q^0)=2}^{(1)} - \hat{r}_k^{(1)} - \hat{r}_{k+q}^{(1)} \right] \\ &= e^{k^2} \left[2 k k \frac{k^2}{3} \mathbf{1} : \hat{r} \hat{v} + k^2 \frac{5}{2} k \hat{r} \ln T \right]; \end{aligned} \quad (18)$$

where $\hat{r} = \frac{p}{\sqrt{2m k_B T}} \frac{\partial f^{(eq)}}{\partial r}$, and we have redefined $\hat{r}^{(1)}$ as a function of $k = \frac{p}{\sqrt{2m k_B T}}$. Similarly, eq. (11) now reads

$$\int \frac{d^3 k}{4\pi^2} e^{k^2} k^n \hat{r}_k^{(1)} = 0 \quad (n = 0, 1, 2); \quad (19)$$

Equation (18) with subsidiary condition (19) forms a linear integralequation for $\hat{r}_k^{(1)}$.

The right-hand side of eq. (18) suggests that we may seek the solution in the form:^{16,17}

$$\begin{aligned} \hat{r}_k^{(1)} &= \ln^{1/3} A^{5/2} (k^2) k k \frac{k^2}{3} \mathbf{1} : \hat{r} \hat{v} \\ &+ A^{3/2} (k^2) k \hat{r} \ln T; \end{aligned} \quad (20)$$

where $A^{5/2}$ and $A^{3/2}$ are two unknown functions; the use of fractions $5/2$ and $3/2$ to distinguish them will be rationalized shortly. Substituting eq. (20) into it, we can transform eq. (18) into separate equations for A as

$$\begin{aligned} & \frac{2}{\pi} \frac{p}{\lambda} \frac{1}{2} \int \frac{d^3 q}{4} \frac{d^3 q^0}{4} \frac{(q^0 - q)}{q} e^{k^2 (k+q)^2} \left[\hat{T}_{k+(q-q^0)=2} + \hat{T}_{k+(q+q^0)=2} - \hat{T}_k - \hat{T}_{k+q} \right] \\ &= e^{k^2} R_k; \end{aligned} \quad (21)$$

where tensor R_k and T_k are defined in Table I together with another tensor W_k . Since the factor e^{-k^2} is present on the right-hand side of eq. (21), we expand $A^{(n)}$ further in the Sonine polynomials $S_n^{(n)}$ as^{16,17}

$$A^{(n)} = \sum_{k=0}^{\infty} c_k S_k^{(n)}; \quad (22)$$

Use of two different complete sets fS, g , ($n=5=2; 3=2$) is only for convenience to transform the right-hand side of eq. (21) into a vector with a single nonzero element. With eq. (20) and (22) and the orthogonality of $S_n^{(n)}$, we find that the constraint (19) reduces to the single condition:

$$c_0^{3=2} = 0; \quad (23)$$

We hence remove the $n=0$ term of $n=3=2$ from eq. (22) in the subsequent discussion. We now take the tensor ($n=5=2$) or the vector ($n=3=2$) product of eq. (21) with $S_n^{(n)}$ (k^2) $W_k = 4$ and perform integration over k . Equation (21) is thereby transformed into an algebraic equation for the expansion coefficients f, g , as

$$\sum_{k=0}^{\infty} T_{k0} c_k = R_n; \quad (24)$$

Here R_n is defined by

$$R_n = \int_0^{\infty} \frac{d^3k}{4} e^{-k^2} S_n^{(n)}(k^2) (W_k; R_k) \\ = \begin{cases} \frac{8}{4} p - n_0 & : n = 5=2 \\ \frac{15p}{16} - n_1 & : n = 3=2 \end{cases}; \quad (25)$$

with $(W_k; R_k) = W_k : R_k$ and $W_k = R_k$ for $n=5=2$ and $3=2$, respectively. Also, T_{k0} is obtained with a change of variable $k \rightarrow q=2$ in the integrals as

$$T_{k0} = \frac{2}{\pi} \int_0^{\infty} \frac{d^3q}{4} e^{-q^2} k^2 \int_0^{\infty} dq e^{-q^2} q^{2=2} q^3 \int_0^{\infty} dq^0 (q^0 - q) \\ I_{n0}(k; q; q) + I_{n0}(k; q; -q) - 2I_{n0}(k; q; q^0); \quad (26)$$

with $I_{n0}(k; q; q^0)$ defined by

$$I_{n0}(k; q; q^0) = \frac{d}{4} \frac{d}{dq^0} S_n^{(n)}((k - q=2)^2) S_0^{(n)}((k - q^0=2)^2) \\ (W_{k, q=2}; W_{k, q^0=2}); \quad (27)$$

TABLE I: Quantities appearing in eq. (21). Here $S_0^{(n)} = 1$ and $S_1^{(n)} = 1 + n$.

	W_k	R_k	T_k
5=2	$k k$	$(k^2=3) \frac{1}{2} S_0(k^2) W_k$	$A(k^2) W_k$
3=2	k	$S_1(k^2) W_k$	$A(k^2) W_k$

The quantities $I_{n0}(k; q; q)$ and $I_{n0}(k; q; -q)$ are obtained from eq. (27) by removing the integral over $d q^0=4$ and setting $q^0 = q$ and $q^0 = -q$ in the integrand, respectively.

The first few series of eq. (26) are easily calculated analytically as $T_{00}^{5=2} = T_{11}^{3=2} = 1$, $T_{01}^{5=2} = T_{12}^{3=2} = 1=4$, $T_{11}^{5=2} = 205=48$ and $T_{22}^{3=2} = 45=16$, in agreement with the values given below eq. (10.21,3) of Chapman and Cowling.¹⁶ The matrix element for a general n can be evaluated numerically. With T_{k0} and R_n thus obtained, eq. (24) is solved by cutting the infinite series at a finite value n_c , and n_c is increased subsequently to check the convergence. Table II lists the values of c_n thereby obtained. Those of $c_0^{5=2}$ and $c_1^{3=2}$ are about 2% larger in magnitude than the analytic ones $5^{5=2}=4$ and $15^{3=2}=16$ with $n_c=0$ and 1 for $n=5=2$ and $3=2$, respectively. This rapid convergence as a function of n_c was already pointed out by Chapman and Cowling.¹⁶

Substituting eqs. (9), (10) and (20) into eqs. (7d) and (7e), we arrive at the first-order contributions to the momentum flux density tensor and the thermal flux density as

$$j_Q^{(1)} = -mn \left(\frac{\partial v_i}{\partial r_j} + \frac{\partial v_j}{\partial r_i} \right) \frac{2}{3} r_{ij} v; \quad (28a)$$

$$j_Q^{(1)} = -\frac{3}{2} n k_B \frac{\partial T}{\partial r}; \quad (28b)$$

respectively, where η and κ are the kinematic viscosity and the thermal diffusivity,^{2,6} respectively, defined by

$$\eta = \frac{1}{4} n \frac{2k_B T}{m} c_0^{5=2}; \quad (29a)$$

$$\kappa = \frac{5}{6} n \frac{2k_B T}{m} c_1^{3=2}; \quad (29b)$$

These quantities clearly have the same dimension. Using them as well as the specific heat at constant pressure C_p and constant volume C_v , we can introduce an important dimensionless quantity $Pr = (\eta = \kappa) (C_p = C_v)$ called the Prandtl number.¹⁶ Adopting $C_p = C_v = 5/3$ of the ideal monatomic gas, we find $Pr = 0.66$ from eq. (29) and Table II, which is in excellent agreement with the value 0.67 for Ar at $T = 273K$.¹⁷ Table III lists values of relevant thermodynamic and transport coefficients around room temperature at 1 atm for Ne, Ar and air.

Thus, we have successfully expressed \underline{j}_Q in terms of n, v and T as eqs. (14), (28) and (29) within the first-order gradient expansion. Now, eq. (8) with eqs. (14),

TABLE II: Values of c_n obtained by solving eq. (24).

	c_0	c_1	c_2	c_3	c_4
5=2	2.2511	0.1390	0.0233	0.0058	0.0018
3=2	0	1.7036	0.1626	0.0371	0.0117

(28) and (29) form a closed set of equations for the variables n, v and T incorporated in $f^{\text{eq}}(p; r; t)$. After solving them, we can obtain the distribution function $f(p; r; t)$ by eqs. (9), (10), (20), (22) and Table II, and subsequently calculate entropy by eq. (6).

III. APPLICATION TO RAYLEIGH-BENARD CONVECTION

We now apply the equations of XII for n, v and T to Rayleigh-Benard convection of a dilute classical monatomic gas confined in the region $-d/2 \leq z \leq d/2$ and $-L/2 \leq x, y \leq L/2$. The gas is heated from below so that

$$T(x; y; z = -d/2) = T_0, \quad T = 2; \quad T > 0: \quad (30)$$

The thickness d and the lateral width L are chosen as $L = d = 1$. It hence follows that (i) there are enough collisions along z and (ii) any effects from the side walls may be neglected. We eventually impose the periodic boundary condition in the xy plane.

We study this system by fixing the total particle number, total energy, and total heat flux through $z = -d/2$. This is equivalent to choosing the average particle density n , the average energy density E , and the average heat flux density j_z at $z = -d/2$ as independent variables; hence $T_0 = T_0(n; E; j_z)$ and $T = T(n; E; j_z)$ in eq. (30). The latter two conditions also imply, due to the energy conservation law, that there is average energy flux density j_z through any cross section perpendicular to z . The fact justifies our choice of j_z as an independent variable to specify the system. It should be noted that this energy flow in the container may be due partly to a macroscopic motion of the gas.

The standard theoretical treatment of Rayleigh-Benard convection starts from introducing the Oberbeck-Boussinesq approximation to the equations for n, v and T .² However, this approximation seems not to have been justified in a widely accepted way. We here develop a systematic approximation scheme for the equations in XII appropriate to treat Rayleigh-Benard convection, which will be shown to yield the equations with the Oberbeck-Boussinesq approximation as the lowest-order approximation. This consideration also enables us to estimate

the entropy change through the convective transition on a macro ground.

A. Introduction of dimensionless units

We first introduce a characteristic temperature T defined by

$$T = E/3nk_B: \quad (31)$$

We then adopt the units where the length, velocity and energy are measured by $d, \sqrt{k_B T/m}$ and $k_B T$, respectively. Accordingly, we carry out a change of variables as

$$t = d \sqrt{\frac{m}{k_B T}} t^0; \quad r = dr^0; \quad (32a)$$

and

$$n = \frac{n^0}{d^3}; \quad v = \sqrt{\frac{k_B T}{m}} v^0; \quad T = T T^0: \quad (32b)$$

Let us substitute eqs. (14), (28) and (29) into eq. (8) and subsequently perform the above change of variables. We thereby obtain the dimensionless conservation laws:

$$\frac{\partial n^0}{\partial t^0} + r^0 \cdot \nabla^0 (n^0 v^0) = 0; \quad (33a)$$

$$n^0 \frac{\partial v^0}{\partial t^0} + n^0 v^0 \cdot \nabla^0 v^0 + r^0 \cdot \nabla^0 P^0 + \sum_i r_i^0 [n^0 \cdot \nabla^0 (r_i^0 v_i^0 + r_i^0 v_i^0)] + \frac{2}{3} r^0 \cdot \nabla^0 (n^0 r^0 \cdot \nabla^0 v^0 + n^0 U_g^0 e_z) = 0; \quad (33b)$$

$$\frac{\partial T^0}{\partial t^0} + v^0 \cdot \nabla^0 T^0 + \frac{1}{n^0} r^0 \cdot \nabla^0 (n^0 r^0 \cdot \nabla^0 T^0) + \frac{2}{3} T^0 r^0 \cdot \nabla^0 v^0 + \frac{2}{3} \sum_{ij} r_i^0 \left[\frac{1}{2} \frac{\partial v_i^0}{\partial r_j^0} + \frac{\partial v_j^0}{\partial r_i^0} \right] - \frac{2}{3} (r^0 \cdot \nabla^0 v^0)^2 = 0; \quad (33c)$$

with $P^0 = n^0 T^0$ and

$$U_g^0 = \frac{r^0 \cdot \nabla^0}{d \sqrt{\frac{m}{k_B T}}}; \quad U_g^0 = \frac{r^0 \cdot \nabla^0}{d \sqrt{\frac{m}{k_B T}}}; \quad U_g^0 = \frac{m g d}{k_B T}: \quad (34)$$

An important dimensionless quantity of the system is the Rayleigh number R defined by

$$R = \frac{U_g^0 T^0}{\alpha^0} = \frac{g T^0 d^3}{\alpha^0}; \quad (35)$$

where T^0 appears as the thermal expansion coefficient of the ideal gas.

The above equations will be solved by fixing $n, E = 3nk_B T = 2$ and j_z , as already mentioned. These conditions are expressed in the dimensionless form as

$$\frac{1}{L^0} \int_{-L^0/2}^{L^0/2} n^0(r^0) d^3 r^0 = n^0; \quad (36a)$$

TABLE III: Values of relevant thermodynamic and transport coefficients under atmospheric pressure given in CGS units [$\alpha = V^{-1}(\partial V / \partial T)$].

	Ne (0°C)	Ar (0°C)	air (0°C)
$m n$	$0.900 \cdot 10^3$	$1.78 \cdot 10^3$	$1.29 \cdot 10^3$
	$3.66 \cdot 10^3$	$3.67 \cdot 10^3$	$3.67 \cdot 10^3$
	$33.0 \cdot 10^2$	$11.8 \cdot 10^2$	$13.2 \cdot 10^2$
	$83.1 \cdot 10^2$	$29.2 \cdot 10^2$	$25.9 \cdot 10^2$

$$\frac{1}{L^2} \int \frac{3}{2} P^0 + \frac{1}{2} n^0 v^0 + n^0 U_g^0 z^0 d^3 r = \frac{3}{2} n^0; \quad (36b)$$

$$\frac{1}{L^2} \int dx^0 dy^0 \frac{3}{2} n^0 \frac{\partial T^0}{\partial z^0} \Big|_{z^0 = \frac{1}{2}} = j_b^0; \quad (36c)$$

where $P^0 = n^0 T^0$, and integrations extend over $L^0=2$ $x^0; y^0$ $L^0=2$ and $z^0 = \frac{1}{2}$ $z^0 = \frac{1}{2}$. Equation (36b) has been obtained by integration of $(p^2=2m + mgz)f$ over r and p with eq. (7), whereas eq. (36c) originates from eq. (28b).

To make an order-of-magnitude estimate for the parameters in eqs. (34) and (35), consider Ar of 273K at 1 atm confined in a horizontal space of d cm with the temperature difference T K. Using Table II, we then obtain the numbers:

$$\begin{aligned} 0 &= 4.95 \cdot 10^6 d; & 0 &= 1.22 \cdot 10^5 d; \\ U_g^0 &= 1.73 \cdot 10^6 d; & T^0 &= 3.67 \cdot 10^3 T; \end{aligned} \quad (37a)$$

and

$$R = 1.04 \cdot 10^2 d^3 T; \quad (37b)$$

The critical Rayleigh number R_c for the convective transition is of the order 10^3 ,² which is realized for $d \approx 2$ cm and $T \approx 1$ K. We now observe that the dimensionless parameters have the following orders of magnitude in terms of 10^3 :

$$0; 0; U_g^0 \approx 2; T^0 \approx 1; R \approx 1; \quad (38)$$

Thus, Rayleigh-Benard convection is a phenomenon where two orders of magnitude (i.e., 0 and 2) are relevant. From now on we shall drop primes in every quantity of eqs. (33) and (36).

B. Omission of the number conservation law

Let us write eq. (33) in terms of $j = nv$ instead of v . It follows from the vector analysis that the vector field j can be written generally as $j = r + r \times A$, where A corresponds to the scalar and vector potentials of the electromagnetic fields, respectively. We then focus in the following only on those phenomena where the current density satisfies $r = 0$, i.e.,

$$r \cdot j = 0; \quad (39)$$

This implies that we may drop eq. (33a) from eq. (33) to treat only eqs. (33b) and (33c).

C. Expansion in

Equation (38) suggests that we may solve eqs. (33b) and (33c) in powers of d . Noting eqs. (36a) and (36b),

we first expand n and T as

$$n = n^{(0)} + \sum_{l=1}^{\infty} n^{(l)}; \quad T = T^{(0)} + \sum_{l=1}^{\infty} T^{(l)}; \quad (40a)$$

With eqs. (29), (34) and (38), we next expand dimensionless parameters $P = (L=4) \frac{P}{2T C_0^{5=2}}$, $U_g = (L=6) \frac{P}{2T C_1^{3=2}}$ and U_g as

$$P = P^{(0)} + \sum_{l=2}^{\infty} P^{(l)}; \quad U_g = U_g^{(0)} + \sum_{l=2}^{\infty} U_g^{(l)}; \quad (40b)$$

where $P^{(2)} = (L=4) \frac{P}{2C_0^{5=2}}$ and $U_g^{(2)} = (L=6) \frac{P}{2C_1^{3=2}}$ are constants with $l = 1(n)$. It also follows from $T^{(1)}$ and eq. (36c) that

$$j_b = j_b^{(3)}; \quad (40c)$$

It remains to attach orders of magnitude to the differential operators and $j = nv$. In this context, we notice that the Oberbeck-Boussinesq approximation yields a critical Rayleigh number R_c which is in good quantitative agreement with experiment.⁷ The fact tells us that the procedure to attach the orders should be carried out so as to reproduce R_c of the Oberbeck-Boussinesq approximation. The requirement yields

$$j = n \sum_{l=1}^{\infty} j^{(l+1=2)}; \quad \frac{\partial}{\partial t} = O(1^{.5}); \quad r = O(0^{.25}); \quad (40d)$$

See eq. (58) below and the subsequent comments for details. The above power-counting scheme will be shown to provide not only a justification of the Oberbeck-Boussinesq approximation but also a systematic treatment to go beyond it.

Let us substitute eq. (40) to eqs. (33b) and (36b). The contributions of $O(1)$ in these equations read $r P^{(1)} = 0$ and $P^{(1)} d^3 r = 0$, respectively, with $P^{(1)} = n(\hat{n}^{(1)} + T^{(1)})$. We hence conclude $P^{(1)} = 0$, i.e.,

$$\hat{n}^{(1)} = -T^{(1)}; \quad (41)$$

It also follows from eqs. (36a) and (36c) with eqs. (40) and (41) that $T^{(1)}$ should obey

$$\sum_{l=2}^{\infty} T^{(l)} d^3 r = 0; \quad (42a)$$

$$\frac{1}{L^2} \sum_{l=2}^{\infty} \int dx \sum_{l=2}^{\infty} dy \frac{\partial T^{(l)}}{\partial z} \Big|_{z=1=2} = \frac{2 j_b^{(3)}}{3 n^{(2)}}; \quad (42b)$$

Equation (42) is still not sufficient to determine $T^{(1)}$. It turns out below that the required equation results from the $O(1^{.3})$ and $O(2^{.5})$ contributions of eqs. (33b) and (33c), respectively.

Next, collecting terms of $O(2)$ in eqs. (33b) and (36b) yield $r P^{(2)} + n U_g^{(2)} e_z = 0$ and $(\frac{3}{2} P^{(2)} + n U_g^{(2)} z) d^3 r =$

0, respectively. Hence $P^{(2)} = -nU_g^{(2)}/z$. Noting $P^{(2)} = n(\hat{n}^{(2)} + \hat{n}^{(1)}T^{(1)} + T^{(2)})$ and using eq. (41), we obtain

$$\hat{n}^{(2)} = (T^{(1)})^2 - T^{(2)} - U_g^{(2)}/z; \quad (43)$$

It follows from eqs. (36a) and (36c) with eqs. (40) and (43) that $T^{(2)}$ should obey

$$[(T^{(1)})^2 - T^{(2)}]d^3r = 0; \quad (44a)$$

$$\int_{L=2}^{\infty} dx \int_{L=2}^{\infty} dy \left[\frac{\partial T^{(2)}}{\partial z} + \frac{T^{(1)}}{2} \frac{\partial T^{(1)}}{\partial z} \right]_{z=1=2} = 0; \quad (44b)$$

In deriving eq. (44b), use has been made of $(n^{(3)})^{(3)} = n^{(2)}T^{(1)}/2$ which results from $1/IT^{1=2}$ and $1/n^{(1)}$; see eqs. (17) and (29b). Equation (44) forms constraints on the higher-order contribution $T^{(2)}$, which will be irrelevant in the present study, however.

Finally, we collect terms of O^{-3} in eq. (33b) to obtain

$$\frac{\partial \hat{j}^{(1;5)}}{\partial t} + \hat{j}^{(1;5)} - \hat{j}^{(1;5)} + \frac{rP^{(3)}}{n} - {}^{(2)}r^2 \hat{j}^{(1;5)} + \hat{n}^{(1)}U_g^{(2)}e_z = 0; \quad (45)$$

where we have used eq. (39). We further operate $r \rightarrow r$ to the above equation and substitute eq. (41). This yields

$$\frac{\partial}{\partial t} r^2 \hat{j}^{(1;5)} + r \hat{j}^{(1;5)} - \hat{j}^{(1;5)} + {}^{(2)}(r^2)^2 \hat{j}^{(1;5)} + U_g^{(2)}(e_z r^2 - e_z r r) \hat{T}^{(1)} = 0; \quad (46a)$$

On the other hand, terms of $O^{-2.5}$ in eq. (33c) lead to

$$\frac{\partial T^{(1)}}{\partial t} + \hat{j}^{(1;5)} - r \hat{T}^{(1)} - {}^{(2)}r^2 T^{(1)} = 0; \quad (46b)$$

Equation (46) forms a set of coupled differential equations for $T^{(1)}$ and $\hat{j}^{(1;5)}$, which should be solved with eq. (42). It is almost identical in form with that derived with the Oberbeck-Boussinesq approximation, predicting the same critical Rayleigh number R_c as will be shown below. The whole considerations on Rayleigh-Bénard convection presented in the following will be based on eq. (46) with eq. (42).

Two comments are in order before closing the subsection. First, if we apply the procedure of deriving eq. (46) to the O^{-4} and $O^{-3.5}$ contributions of eqs. (33b) and (33c), respectively, we obtain coupled equations for the next-order quantities $T^{(2)}$ and $\hat{j}^{(2;5)}$, which should be solved with eq. (44). Thus, we can treat higher-order contributions systematically in the present expansion scheme. Second, eq. (45) may be regarded as the equation to determine $P^{(3)}$ for given $T^{(1)}$ and $\hat{j}^{(1;5)}$. It yields a relation between $T^{(3)}$ and $\hat{n}^{(3)}$, which in turn leads to the constraint for $T^{(3)}$ upon substitution into eqs. (36a) and (36c). On the other hand, the equation for $T^{(3)}$ originates from the O^{-5} and $O^{-4.5}$ contributions of eqs. (33b) and (33c), respectively. Now, one may understand the hierarchy of the approximation clearly.

D. Expression of entropy

We now write down the expression of entropy in powers of ϵ . Entropy of the system can be calculated by eq. (6), where the distribution function f is given by eq. (9) with eqs. (10) and (20). Hereafter we shall drop the superscript in $\epsilon^{(1)}$, which specifies the order in the gradient expansion, to remove possible confusion with the expansion of eq. (40). Thus, f is now expressed as $f = f^{(eq)}(1 + \epsilon)$.

We first focus on ϵ and write eq. (20) in the present units with noting eq. (16). We then realize that ϵ is proportional to $\ln T$ or $\ln v$, which are quantities of O^{-3} and $O^{-3.5}$ in the expansion scheme of eq. (40), respectively. It hence follows that there is no contribution of O^{-2} from ϵ . In contrast, $f^{(eq)}$ yields terms of O^{-2} , as seen below. Thus, we only need to consider $f^{(eq)}$.

Let us write $f^{(eq)}$ of eq. (10) in the present units, substitute eq. (40) into it, and expand the resulting expression in powers of ϵ . We also drop terms connected with j (i.e., v) which have vanishing contribution to S within O^{-2} after the momentum integration in eq. (6). We thereby obtain the relevant expansion:

$$f^{(eq)} = \frac{(2\pi)^{3/2} n}{(2\pi)^{3/2}} e^{-\frac{X^2}{2}} \left[1 + \frac{X^2}{2} \hat{n}^{(1)} + \frac{X^2}{2} \hat{T}^{(1)} + u^{(1)}(\epsilon) \hat{T}^{(1)} + u^{(2)}(\epsilon) (\hat{T}^{(1)})^2 \right]; \quad (47)$$

where $\epsilon = p^2/2$, and $u^{(1)}$ and $u^{(2)}$ are defined by

$$u^{(1)}(\epsilon) = \frac{3}{2}; \quad u^{(2)}(\epsilon) = \frac{1}{2} \epsilon^2 - 5\epsilon + \frac{15}{4}; \quad (48)$$

Let us substitute eq. (47) into eq. (6) and carry out integration over p . The contribution of O^{-1} is easily obtained as ($k_B = 1$)

$$S^{(0)} = n \ln \frac{(2\pi)^{3/2}}{(2\pi)^{3/2} n} + \frac{5}{2}; \quad (49)$$

which is just the equilibrium expression¹⁹ for density n and temperature T in the conventional units, as it should. Next, we find $S^{(1)} = 0$ due to eqs. (41) and (42a). Thus, the contribution characteristic of heat conduction starts from the second order. A straightforward calculation yields

$$S^{(2)} = \frac{5}{4V} \int d^3r T^{(1)2}; \quad (50)$$

Equation (50) is the basic starting point to calculate the entropy change through the convective transition. Note that we have fixed j_0 in the present consideration, i.e., the initial temperature slope as seen from eq. (42b).

At this state, it may be worthwhile to present a qualitative argument on entropy of Rayleigh-Bénard convection.

With the initial temperature profile fixed as eq. (42b), eq. (50) tells us that entropy will be larger as the temperature profile becomes more uniform between $z = -1$ to $z = 1$. The conducting state with $v = 0$ has the linear temperature profile, as shown shortly below in eq. (52). Thus, any increase of entropy over this conducting state is brought about by reducing the temperature difference between $z = -1$ to $z = 1$. Such a state necessarily accompanies a temperature variation which is weaker around $z = 0$ than near the boundaries $z = -1$ to $z = 1$. This temperature profile is indeed an essential feature of Rayleigh-Bénard convection which show up as an increase of the Nusselt number (i.e., the efficiency of heat transport) under fixed temperature difference.^{2,7} Combining eqs. (42b) and (50) with the experimental observation on the Nusselt number, we thereby conclude without any detailed calculations that entropy of Rayleigh-Bénard convection should be larger than entropy of the conducting state in the present conditions with $j_0 = \text{const.}$ Thus, Rayleigh-Bénard convection is expected to satisfy the principle of maximum entropy given at the beginning of the paper. We shall confirm this fact below through detailed numerical studies.

IV. PERIODIC SOLUTION WITH STRESS-FREE BOUNDARIES

Equation (46) with eq. (42) forms a set of simultaneous equations for $T^{(1)}$ and $\hat{j}^{(1,5)}$, which should be supplemented by the boundary condition on $\hat{j}^{(1,5)}$. For simplicity, we here adopt the assumption of stress-free boundaries:²

$$\hat{j}_z^{(1,5)} = \frac{\partial^2}{\partial z^2} \hat{j}_z^{(1,5)} = 0 \quad \text{at } z = \pm \frac{1}{2} : \quad (51)$$

However, qualitative features of the convective solutions will be universal among the present and more realistic/complicated boundary conditions; see the argument at the end of the preceding section.

We first discuss the heat-conducting solution of eq. (46) and its instability towards convection. We then transform eq. (46) with eqs. (42) and (51) in a form suitable to obtain periodic convective structures.

A. Conducting solution

Let us consider the conducting solution of eq. (46) where $\hat{j}^{(1,5)} = 0$ with uniformity in the xy plane. Equation (46) then reduces to $d^2 T^{(1)} / dz^2 = 0$, which is solved with eq. (42) as

$$T^{(1)} = T_{hc} z; \quad T_{hc} = \frac{2j_0^{(3)}}{3n^{(2)}} : \quad (52)$$

Substituting this expression into eq. (50), we obtain entropy of the conducting state measured from $S^{(0)}$ as

$$S_{hc}^{(2)} = \frac{5}{48} (T_{hc})^2 : \quad (53)$$

B. Instability of the conducting state

We next check stability of the conducting solution by adding a small perturbation given by

$$\hat{j}^{(1,5)}(r; t) = e^{t e^{ik_z r}} (j^s \sin k_z + j^c \cos k_z); \quad (54a)$$

$$T^{(1)}(r; t) = T_{hc} z + T e^{t e^{ik_z r}} \sin k_z; \quad (54b)$$

where $z = -1$ to $z = 1$, $k_z = \sqrt{3}$ ($\sqrt{3} = 1; 2$) from eq. (51), and j^c denotes a vector in the xy plane. Let us substitute eq. (54) into eq. (46) and linearize it with respect to the perturbation. This leads to

$$(\frac{1}{2} + (2)k^2)k^2 j^s - U_g^{(2)} k_z^2 T e_z = 0; \quad (55a)$$

$$(\frac{1}{2} + (2)k^2)k^2 j^c - i U_g^{(2)} k_z T = 0; \quad (55b)$$

$$(\frac{1}{2} + (2)k^2) T - T_{hc} j^c = 0; \quad (55c)$$

The components j^s and j^c in the xy plane are obtained from eqs. (55a) and (55b) as

$$j^s = 0; \quad j^c = \frac{i U_g^{(2)} k_z k_z}{(\frac{1}{2} + (2)k^2)k^2} T; \quad (56)$$

In contrast, the z component of eq. (55a) and eq. (55c) form linear homogeneous equations for j^c and T . The requirement that they have a non-trivial solution yields

$$2 + (\frac{1}{2} + (2))k^2 + (2)(2)(k^4 - R^{(1)} k_z^2 - k^2) = 0; \quad (57)$$

with $R^{(1)}$ the Rayleigh number defined by eq. (35) with $U_g^0 = U_g^{(2)}$, $T = T_{hc}$, $0 = (2)$ and $0 = (2)$. The conducting solution becomes unstable when eq. (57) has a positive solution, i.e.,

$$R^{(1)} = \frac{U_g^{(2)} T_{hc}}{(2)(2)} = \frac{(k_z^2 + k_z^2)^3}{k_z^2} = \frac{27}{4} : \quad (58)$$

Thus, we have obtained the value $R_c = 27/4 = 4$ for the critical Rayleigh number^{2,3} which corresponds to $(k_z; k_z) = (\sqrt{2}; \sqrt{2})$.

Besides reproducing the established results,² the above consideration may also be important in the following respects. First, we require that: (i) terms of the z component of eq. (55a) all have the same order in T with $T = 0$ (); (ii) the same be true for terms of eq. (55c). This leads to the attachment of the order-of-magnitude: $j = O(1^{1,5})$, $k = O(0^{2,5})$ and $\theta = O(1^{1,5})$, thereby justifying eq. (40d). The conclusion $k = O(0^{2,5})$ also results from $k = \frac{1}{3} = \frac{1}{3} = \frac{1}{3}$ for the critical Rayleigh number. Second, eq. (58) removes the ambiguity in k , and to estimate the critical Rayleigh number R_c . Specifically, we should use the mean values over $-1 \leq z \leq 1$ for a detailed comparison of R_c between theory and experiment.

C. Convective solution

We now focus on the convective solution of eq. (46) with periodic structures. Let us introduce basic vectors as

$$\mathbf{a}_1 = (a_{1x}; a_{1y}; 0); \quad \mathbf{a}_2 = (0; a_2; 0); \quad \mathbf{a}_3 = \mathbf{e}_z; \quad (59)$$

We consider the region in the xy plane spanned by $N_1 \mathbf{a}_1$ and $N_2 \mathbf{a}_2$ with N_j ($j = 1; 2$) a huge integer, and impose the periodic boundary condition. The wave vector \mathbf{k} is then defined in terms of the reciprocal lattice vectors $\mathbf{b}_1 = 2\pi(\mathbf{a}_2 \times \mathbf{a}_3) = [a_1 \ a_2 \ 0]$, $\mathbf{b}_2 = 2\pi(\mathbf{a}_3 \times \mathbf{a}_1) = [0 \ a_2 \ a_1]$ and $\mathbf{b}_3 = \mathbf{e}_z$ as

$$\mathbf{k} = \sum_{j=1}^3 j \mathbf{b}_j; \quad (60)$$

with j denoting an integer. The analysis of XIV B suggests that the stable solution satisfies $j_1 j_2 j_3 = 2$.

Equation (56) tells us that j_2 and T are out-of-phase. Also noting eqs. (42) and (51), we now write down the steady solution of eq. (46) in the form:

$$j_2^{(1;5)}(\mathbf{r}) = \sum_{\mathbf{k}_2 \in \mathbf{G}_2} \sum_{\mathbf{k}} j_{2k} \sin(\mathbf{k}_2 \cdot \mathbf{r}) \cos_{\mathbf{k}}; \quad (61a)$$

$$j_2^{(1;5)}(\mathbf{r}) = \sum_{\mathbf{k}_2 \in \mathbf{G}_2} \sum_{\mathbf{k}} j_{2k} \cos(\mathbf{k}_2 \cdot \mathbf{r}) \sin_{\mathbf{k}}; \quad (61b)$$

$$T^{(1)}(\mathbf{r}) = \sum_{\mathbf{k}_2 \in \mathbf{G}_2} \sum_{\mathbf{k}} T_k \cos(\mathbf{k}_2 \cdot \mathbf{r}) \sin_{\mathbf{k}} + T_{cv} z + T_1; \quad (61c)$$

where $z + 1 = 2$, and we have chosen $j_2^{(1;5)}$ and $T^{(1)}$ as even functions in the xy plane without losing the generality. The \mathbf{k} summations in eq. (61) run over

$$\begin{pmatrix} 1 & 1 & 1 \\ 0 & 1 & 1 \end{pmatrix}; \begin{pmatrix} 1 & 1 & 1 \\ 0 & 2 & 1 \end{pmatrix}; \begin{pmatrix} 1 & 1 & 1 \\ 1 & 1 & 1 \end{pmatrix}; \begin{pmatrix} 1 & 1 & 1 \\ 1 & 2 & 1 \end{pmatrix}; \begin{pmatrix} 1 & 1 & 1 \\ 1 & 3 & 1 \end{pmatrix}; \quad (62)$$

which covers all the independent basis functions. The condition (39) is transformed into

$$k j_{2k} + k_z j_{zk} = 0; \quad (63a)$$

Thus, j_{2k} may be written generally as

$$j_{2k} = \frac{k_2 k_z}{k_2^2} j_{zk} + \frac{e_z k_2}{k_2} j_{pk}; \quad (63b)$$

The constants T_{cv} and T_1 in eq. (61c) denote the temperature difference between $z = 1=2$ and the average temperature shift, respectively. They are fixed so as to satisfy eq. (42) as

$$T_{cv} = T_{hc} + \sum_{\mathbf{k}_z} T_{k_2=0, k_z} k_z; \quad (64a)$$

$$T_1 = \sum_{\mathbf{k}_z} T_{k_2=0, k_z} \frac{1}{k_z} \cos k_z; \quad (64b)$$

where T_{hc} denotes temperature difference of the conducting state given explicitly in eq. (52).

It follows from the energy conservation law that eq. (42b) should also hold at $z = 1=2$, which leads to an alternative expression for T_{cv} . Subtracting it from eq. (64a) yields the identity obeyed by $T_{k_2=0, k_z}$:

$$\sum_{\mathbf{k}_z} T_{k_2=0, k_z} k_z (1 - \cos k_z) = 0; \quad (65)$$

which is useful to check the accuracy of numerical calculations.

Let us substitute eq. (61) into eq. (46). A straightforward calculation of using eq. (63) then leads to coupled algebraic equations for T_k , j_{zk} and j_{pk} as

$$\begin{aligned} & (2) k^2 T_k - T_{cv} j_{zk} \\ & + \frac{1}{4} \sum_{\mathbf{k} \in \mathbf{G}_0} T_{k^0} k j_{k^0} (k_2^0 + k_2^0 k_2 + k_z^0 k_z^0 k_z) \\ & + (k_2^0 + k_2^0 k_2 + k_z^0 + k_z^0 k_z) + \frac{1}{2} \frac{k_z^0}{2} (k_2^0 k_2^0 k_2 + k_z^0 + k_z^0 k_z) \\ & + k_2^0 k_2^0 k_2 + k_z^0 k_z^0 k_z + k_2^0 k_2^0 k_2 + k_z^0 k_z^0 k_z \\ & + k_2^0 j_{2k^0} k_z j_{zk^0} (k_2^0 + k_2^0 k_2 + k_z^0 k_z^0 k_z) \\ & + \frac{1}{2} \frac{k_z^0}{2} (k_2^0 k_2^0 k_2 + k_z^0 k_z^0 k_z) + k_2^0 k_2^0 k_2 + k_z^0 k_z^0 k_z \\ & = 0; \end{aligned} \quad (66a)$$

$$\begin{aligned} & (2) k^2 j_{zk} - U_g^{(2)} \frac{k_z^2}{k^2} T_k \\ & + \frac{1}{4} \sum_{\mathbf{k} \in \mathbf{G}_0} j_{zk^0} k j_{k^0} (k_2^0 + k_2^0 k_2 + k_z^0 k_z^0 k_z) \\ & + (k_2^0 k_2^0 k_2 + k_z^0 + k_z^0 k_z) + k_2^0 k_2^0 k_2 + k_z^0 k_z^0 k_z \\ & + k_2^0 k_2^0 k_2 + k_z^0 k_z^0 k_z + k_2^0 k_2^0 k_2 + k_z^0 k_z^0 k_z \\ & + (k_2^0 j_{2k^0} k_z j_{zk^0}) (k_2^0 k_2^0 k_2 + k_z^0 k_z^0 k_z) \\ & + k_2^0 k_2^0 k_2 + k_z^0 k_z^0 k_z + k_2^0 k_2^0 k_2 + k_z^0 k_z^0 k_z \\ & + \frac{k_z}{4k^2} \sum_{\mathbf{k} \in \mathbf{G}_0} (k_2^0 j_{2k^0} k_z j_{zk^0}) k j_{k^0} \\ & (k_2^0 + k_2^0 k_2 + k_z^0 k_z^0 k_z + k_2^0 k_2^0 k_2 + k_z^0 k_z^0 k_z) \\ & + k j_{k^0} k j_{k^0} (k_2^0 + k_2^0 k_2 + k_z^0 k_z^0 k_z) \\ & + k_2^0 k_2^0 k_2 + k_z^0 k_z^0 k_z + k_2^0 k_2^0 k_2 + k_z^0 k_z^0 k_z \\ & (k_2^0 j_{2k^0} k_z j_{zk^0}) (k_2^0 j_{2k^0} k_z j_{zk^0}) \\ & (k_2^0 k_2^0 k_2 + k_z^0 k_z^0 k_z + k_2^0 k_2^0 k_2 + k_z^0 k_z^0 k_z) \\ & + k j_{k^0} k (k_2^0 j_{2k^0} k_z j_{zk^0}) (k_2^0 + k_2^0 k_2 + k_z^0 k_z^0 k_z) \\ & (k_2^0 k_2^0 k_2 + k_z^0 k_z^0 k_z) = 0; \end{aligned} \quad (66b)$$

$$\begin{aligned}
(2)k^2\tilde{j}_{pk} + \frac{1}{4} \sum_{k^0 k^0} \frac{(e_z - k_z) \tilde{j}_{2k^0}}{k_z} k \tilde{j}_{k^0} \\
+ (k_z^0 + k_z^0 k_z - k_z^0 k_z^0 k_z - k_z^0 k_z^0 k_z - k_z^0 k_z^0 k_z - k_z^0 k_z^0 k_z) \\
+ (k_z^0 k_z^0 k_z - k_z^0 k_z^0 k_z - k_z^0 k_z^0 k_z - k_z^0 k_z^0 k_z) \\
+ (k_z^0 k_z^0 k_z - k_z^0 k_z^0 k_z - k_z^0 k_z^0 k_z - k_z^0 k_z^0 k_z) \\
+ (k_z^0 k_z^0 k_z - k_z^0 k_z^0 k_z - k_z^0 k_z^0 k_z - k_z^0 k_z^0 k_z) = 0; \quad (66c)
\end{aligned}$$

with \tilde{j}_{2k} given by eq. (63b). Finally, entropy in convection is obtained from eqs. (50) and (61c) as

$$\begin{aligned}
S_{cv}^{(2)} = \frac{5}{4} \frac{(T_{cv})^2}{12} T_1^2 + \frac{1}{4} \sum_k \tilde{j}_k^2 (1 + k_z^0) \\
+ T_{cv} \sum_{k_z} T_{k_z=0; k_z} \frac{1 + \cos k_z}{k_z} : \quad (67)
\end{aligned}$$

V. NUMERICAL RESULTS

We now present numerical results on entropy of Rayleigh-Benard convection obtained by solving eqs. (66a)–(66c). As a model system we consider Ar at $T = 273K$ under atmospheric pressure and use the values (37) for the parameters in eqs. (66a)–(66c). We also fix the heat flux density j_0 at $z = d/2$ so that temperature difference T_{hc} of the conducting state, expressed in terms of j_0 as eq. (52), takes the value $T_{hc} = 1K$. The Rayleigh number $R^{(1)}$ is then controlled by changing the thickness d . We here adopt the units described above eq. (32) with $k_B = 1$.

Recent experiments on Rayleigh-Benard convection have been performed most actively with compressed classical gases^{5,8,9} where controlled optical measurements of convective patterns are possible. It has been pointed out that the basic n (l^1) and T dependences of eq. (29) are well satisfied even for those gases under high pressures.⁸ Thus, the present consideration with eq. (37) has direct relevance to those experiments.

A. Numerical procedures

To solve the coupled equations numerically, we first multiply eqs. (66a)–(66c) by 10^8 , 10^{10} and 10^{10} , respectively, and rewrite them in terms of $T_k^0 = 10^3 T_k$ and $\tilde{j}_k^0 = 10^5 \tilde{j}_k$ to obtain equations of $O(1)$. We next replace zeros of the right-hand sides by $\partial T_k^0 / \partial t^0$, $\partial \tilde{j}_{2k}^0 / \partial t^0$ and $\partial \tilde{j}_{pk}^0 / \partial t^0$, respectively. These time derivatives are what one would get by retaining time dependence in the expansion coefficients of eq. (61). We then discretize the time derivatives as $\partial T_k^0(t^0) / \partial t^0 = (T_k^0(t^0 + \Delta t^0) - T_k^0(t^0)) / \Delta t^0$, for example. The summations over k are truncated by using a finite value Δ_c (≈ 5) in place of 1 in eq. (62).

As for periodic structures, we investigate the three candidates: the roll, the square lattice and the hexagonal lattice with $j_1 = j_2 = 2$. With these preliminaries, we trace time evolution of the expansion coefficients until they all acquire constant values. Choosing $t^0 = 0.005$ and $\Delta_c = 5$ yields excellent convergence for the calculations presented below. The initial state is chosen as the conducting state with small fluctuations $T_k^0 = 10^2$ for the basic harmonics k . The constants T_{cv} and T_1 have been updated at each time step by using eq. (64). Also evaluated at each time step is entropy measured with respect to the heat-conducting state:

$$S = S_{cv}^{(2)} - S_{hc}^{(2)}; \quad (68)$$

where $S_{hc}^{(2)}$ and $S_{cv}^{(2)}$ are given by eqs. (53) and (67), respectively. We thereby trace time evolution of S simultaneously. The above procedure is carried out for each fixed periodic structure.

We have studied the range: $1 \leq R^{(1)} \leq 10$. Although the region extends well beyond the Busse balloon^{3,6} of stability for classical gases,^{5,8,9} it will be worth clarifying the basic features of steady periodic solutions over a wide range of the Rayleigh number.

B. Results

Figure 1 plots S as a function of t^0 for the Rayleigh number $R^{(1)} = 1.2R_c$ which is slightly above the critical value $R_c = 27.4 = 4$. The letters r , s and h denote (r)

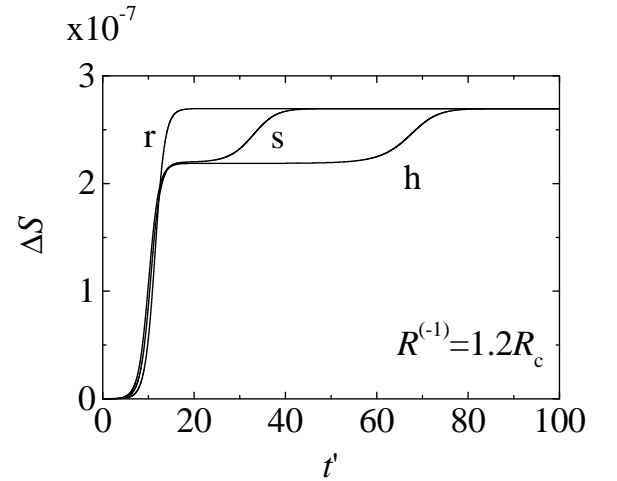


FIG. 1: Time evolution of entropy measured with respect to the heat-conducting state for $R^{(1)} = 1.2R_c$. The letters r , s and h denote roll, square and hexagonal, respectively, distinguishing initial fluctuations around the heat-conducting solution; see text for details. The final state of $t^0 \approx 80$ is the roll convection, whereas the intermediate plateaus of s and h correspond to the square and hexagonal convections, respectively.

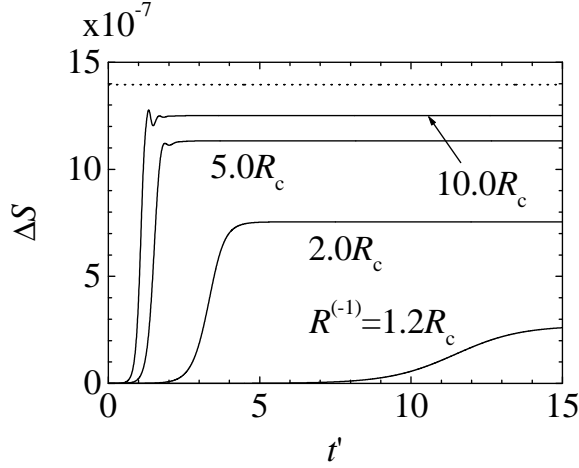


FIG. 2: Time evolution of entropy S . The four curves correspond to the different Rayleigh numbers: $R^{(1)} = 1.2R_c$, $2.0R_c$, $5.0R_c$ and $10.0R_c$. The initial state is the heat-conducting state with the fluctuation $T^0[1;0;1] = 1.0 \cdot 10^{-2}$ and $b_1 = b_2 = \frac{1}{2}$, whereas all the final states are the roll convection. The broken line near the top indicates the upper bound of S .

roll, (s) square and (h) hexagonal, respectively, distinguishing initial conditions. Writing $T_k^0 = T^0[1;2;3]$ and introducing the angle by $\cos(\phi_1, \phi_2)$, those initial conditions are given explicitly as follows: (r) $T^0[1;0;1] = 1.00 \cdot 10^{-2}$ with $b_1 = b_2 = \frac{1}{2}$; (s) $T^0[1;0;1] = 1.01 \cdot 10^{-2}$ and $T^0[0;1;1] = 0.99 \cdot 10^{-2}$ with $b_1 = b_2 = \frac{1}{2}$ and $\phi_1 = \phi_2 = 2$; (h) $T^0[1;0;1] = T^0[0;1;1] = 1.00 \cdot 10^{-2}$ and $T^0[1;1;1] = 1.01 \cdot 10^{-2}$ with $b_1 = b_2 = \frac{1}{2}$ and $\phi_1 = \phi_2 = 3$. We observe clearly that entropy increases monotonically in all the three cases to reach a common final value, which is identified as the roll convection. Thus, the law of increase of entropy is well satisfied even in the open driven system of Rayleigh-Bénard convection under the condition of fixed mechanical variables, i.e., particle number, volume, energy and energy flux. The intermediate plateaus seen in s and h correspond to the metastable square and hexagonal lattices, respectively, with (s) $T^0[1;0;1] = T^0[0;1;1]$ and (h) $T^0[1;0;1] = T^0[0;1;1] = T^0[1;1;1]$. The escapes from those lattice structures are brought about by the tiny initial asymmetry between (s) $T^0[1;0;1]$ and $T^0[0;1;1]$ and (h) $T^0[1;0;1] = T^0[0;1;1]$ and $T^0[1;1;1]$, to form eventually the roll convection of (s) $T^0[0;1;1] = 0$ and (h) $T^0[1;0;1] = T^0[0;1;1] = 0$. Indeed, those escapes are absent if we choose (s) $T^0[1;0;1] = T^0[0;1;1]$ and (h) $T^0[1;0;1] = T^0[0;1;1] = T^0[1;1;1]$ at $t^0 = 0$. We have also performed the same calculations for different initial values of $T^0[1;0;1]$, $T^0[0;1;1]$, $T^0[1;1;1] = 10^{-6} \cdot 10^{-2}$. The smaller initial fluctuations merely delay the first steep rise in S with no observable quantitative changes thereafter.

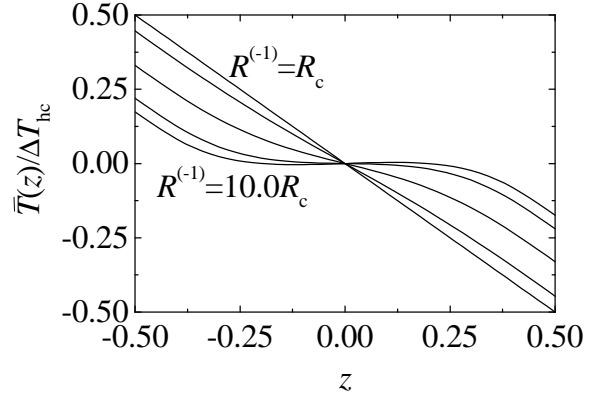


FIG. 3: Profile of the average temperature variation $T(z)$ in the roll convection normalized by the temperature difference T_{hc} in the heat-conducting state. The Rayleigh numbers are $R^{(1)} = R_c, 1.2R_c, 2.0R_c, 5.0R_c$ and $10.0R_c$ from top to bottom on the left part.

Thus, we have confirmed that the roll convection is stable for the infinite horizontal area, which was predicted originally by Schlüter, Lortz and Busse²⁰ for $R > R_c$ based on the linear stability analysis; see also refs. 3 and 7. It should be noted at the same time that the entropy differences among different structures are rather small. We hence expect that: (i) the order of the stability may easily be changed by finite-size effects, boundary conditions, etc.; (ii) initial conditions, fluctuations and defects play important roles in Rayleigh-Bénard convection. These are indeed the features observed experimentally.^{5,8,9}

Figure 2 plots time evolution of S for four different Rayleigh numbers, all developing from the initial fluctuation $T^0[1;0;1] = 1.00 \cdot 10^{-2}$ with $b_1 = b_2 = \frac{1}{2}$. Each final state is the roll convection, which is stabilized faster as $R^{(1)}$ becomes larger. The increase in S is seen quite steep for $R^{(1)} = 10R_c$ followed by a small oscillation. This oscillation in S may be due either to (i) the fluctuations in particle number, momentum, energy and energy flux inherent to open systems or (ii) the initial correlations which causes the anti-kinetic evolution.^{21,22} Such fluctuations are also observed in a numerical study by Orban and Bellemans^{21,22} for an isolated system and not in contradiction with the law of increase of entropy. We observe clearly that the principle of maximum entropy proposed at the beginning of xI, which is relevant to the final steady state without time evolution, is indeed satisfied here. The dotted line in Fig. 2 is the upper bound of entropy in convection, as may be realized from eq. (50). As the Rayleigh number is increased further, entropy differences between different structures become smaller so that the system will eventually fall into the region where fluctuations dominate with no stable structure. The turbulence observed in this region^{3,6,9} may be connected with this instability.

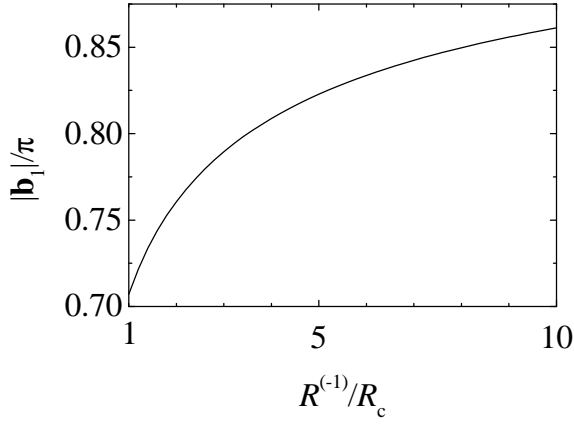


FIG. 4: The length $|b_1|$ of the stable roll convection as a function of the normalized Rayleigh number $R^{(1)}/R_c$. Here $|b_1| = \sqrt{2}$ at $R^{(1)}/R_c = 1$.

Figure 3 shows a profile of the average temperature variation $T(z)$ along z in the roll convection for various Rayleigh numbers. Temperature has less variation as the Rayleigh number becomes larger, thereby increasing entropy of the system. Thus, we may attribute the formation of convection to its efficiency for increasing entropy under fixed inflow of heat, i.e., the initial slope of temperature. Experiments on Rayleigh-Bénard convection have naturally been carried out by fixing the temperature difference rather than the inflow of heat, and formation of the convection has been discussed in terms of the change in the Nusselt number^{2,7} (i.e., the efficiency of the heat transport) due to the increase of the initial temperature slope through the convective transition. Here we have seen that the same phenomenon can be explained with respect to the basic thermodynamic quantity of entropy. Thus, the principle of maximum entropy partly justifies the maximum heat transfer hypothesis by Malkus and Veronis.²³

All the above calculations have been carried out by fixing the periodic structure. They clearly show that the principle of maximum entropy is indeed obeyed. We now take the principle as granted and use it to determine the stable lattice structure. We carry this out within the roll convection by changing the value $|b_1|$.

Figure 4 plots $|b_1|$ as a function of normalized Rayleigh number $R^{(1)}/R_c$. As seen clearly, $|b_1|$ increases gradually from the value $\sqrt{2}$ at $R^{(1)}/R_c = 1$. This tendency is in qualitative agreement with the experiment by Hu, Ecke and Ahlers²⁴ using a circular cell of $L/d = 1$; see also ref. 9. It should be noted at the same time that the entropy difference around $|b_1| = \sqrt{2}$ is quite small. For

example, the stable state for $R^{(1)}/R_c = 10$ corresponds to $|b_1| = 0.829$, but entropy is increased by only 2×10^{-9} from the value $S = 1.296 \times 10^{-6}$ at $|b_1| = \sqrt{2}$. Hence it is expected that (i) initial conditions, fluctuations and boundary conditions play important roles and (ii) it may take a long time, or even be impossible in certain cases, to reach the stable state. These are indeed in agreement with experimental observations.^{5,8,9}

The whole our results have been obtained for the stress-free boundary condition (51). However, the qualitative results will be valid also for more realistic boundary conditions. Indeed, experiments on Rayleigh-Bénard convection all exhibit the temperature profile with a steep change near the boundaries followed by moderate variation in the bulk region as reflected in the enhancement of the Nusselt number.^{2,7} And it is this feature in the present study which has caused increase of entropy in convection over that in the conducting state.

VI. CONCLUDING REMARKS

The present study shows unambiguously that the principle of maximum entropy given at the beginning of XI is indeed satisfied through the Rayleigh-Bénard convective transition of a dilute classical gas. The result is encouraging for the principle as a general rule to determine the stability of nonequilibrium steady states. We need to investigate other open systems, as well as Rayleigh-Bénard convection without fixing the lattice structure, to confirm its validity further.

It may be worth emphasizing once again that entropy/probability, which is the central concept of equilibrium thermodynamics/statistical mechanics, seems to have been left out of the investigations on nonequilibrium systems and pattern formation. Indeed, they have been almost always based on deterministic equations closely connected with conservation laws.⁶ Calculations of entropy for open driven systems inply treating those nonequilibrium systems as subjects of statistical mechanics with considering the boundary conditions explicitly. Those calculations are expected to shed new light on nonequilibrium phenomena in general which are still mysterious.

Acknowledgments

The author is grateful to H. R. Brand for useful and informative discussions on Rayleigh-Bénard convection. This work is supported in part by the 21st century COE program "Topological Science and Technology," Hokkaido University.

¹ T. Kita: J. Phys. Soc. Jpn. 75 (2006) 114005.

² S. Chandrasekhar: Hydrodynamic and Hydromagnetic Sta-

- bility (Clarendon Press, Oxford, 1961).
- ³ F. H. Busse: Rep. Prog. Phys. 41 (1978) 1929.
 - ⁴ R. P. Behringer: Rev. Mod. Phys. 57 (1985) 657.
 - ⁵ V. Croquette: Compt. Phys. 30 (1989) 113; 30 (1989) 153.
 - ⁶ M. C. Cross and P. C. Hohenberg: Rev. Mod. Phys. 65 (1993) 851.
 - ⁷ E. L. Koschmieder: Benard cells and Taylor vortices (Cambridge Univ. Press, Cambridge, 1993).
 - ⁸ J. R. de Bruyn, E. Bodenschatz, S. W. Morris, S. P. Trainor, Y. Hu, D. S. Cannell and G. Ahlers: Rev. Sci. Instrum. 67 (1996) 2043.
 - ⁹ E. Bodenschatz, W. Pesch and G. Ahlers: Annu. Rev. Fluid Mech. 32 (2000) 709.
 - ¹⁰ D. D. Joseph: J. Fluid Mech. 47 (1971) 257.
 - ¹¹ E. A. Spiegel and G. Veronis: Astrophys. J. 131 (1960) 442; 135 (1962) 655.
 - ¹² J. M. Mahajan: Astrophys. J. 136 (1962) 1126.
 - ¹³ R. P. Cordon and M. G. Velarde: J. Phys. (Paris) 36 (1975) 591; 37 (1976) 177.
 - ¹⁴ D. D. Gray and A. Giorgini: Int. J. Heat Mass Transfer. 19 (1976) 545.
 - ¹⁵ K. R. Rajagopal, M. Ruzicka and A. R. Srinivasa: Math. Mod. Meth. Appl. Sci. 6 (1996) 1157.
 - ¹⁶ S. Chapman and T. G. Cowling: The Mathematical Theory of Non-uniform Gases (Cambridge University Press, Cambridge, 1990).
 - ¹⁷ J. O. Hirschfelder, C. F. Curtiss and R. B. Bird: Molecular Theory of Gases and Liquids (Wiley, New York, 1954).
 - ¹⁸ L. D. Landau and E. M. Lifshitz: Mechanics (Pergamon, New York, 1976) x18.
 - ¹⁹ F. Reif: Fundamentals of statistical and thermal physics (McGraw-Hill, New York, 1965) x73.
 - ²⁰ A. Schluter, D. Lortz and F. Busse: J. Fluid Mech. 23 (1965) 129.
 - ²¹ J. Orban and A. Bellemans: Phys. Lett. 24A (1967) 620.
 - ²² C. Cercignani: Ludwig Boltzmann: The Man Who Trusted Atoms (Oxford Univ., Oxford, 1998) x54.
 - ²³ W. V. R. Malkus and G. Veronis: J. Fluid Mech. 4 (1958) 225.
 - ²⁴ Y. Hu, R. Ecke and G. Ahlers: Phys. Rev. E 48 (1993) 4399.